THE JOURNAL OF BIOLOGICAL CHEMISTRY
Vol. 277, No. 15, Issue of April 12, pp. 13129–13137, 2002
Printed in U.S.A.

Structural and Functional Analyses of DM43, a Snake Venom Metalloproteinase Inhibitor from *Didelphis marsupialis* Serum*

Received for publication, January 18, 2002
Published, JBC Papers in Press, January 28, 2002, DOI 10.1074/jbc.M200589200

Ana G. C. Neves-Ferreira‡, Jonas Perales‡, Jay W. Fox§, John D. Shannon§, Débora L. Makino¶, Richard C. Garratt¶, and Gilberto B. Domont‖**

From the ‡Departamento de Fisiologia e Farmacodinâmica, Instituto Oswaldo Cruz, Fiocruz, 21045-900 Rio de Janeiro, Brazil, the §Department of Microbiology, University of Virginia, Charlottesville, Virginia 22908, the ¶Departamento de Física e Informática, Instituto de Física de São Carlos, Universidade de São Paulo, São Carlos, 13566-590 São Paulo, Brazil, and the ‖Departamento de Bioquímica, Instituto de Química, Universidade Federal do Rio de Janeiro, 21949-900 Rio de Janeiro, Brazil

DM43, an opossum serum protein inhibitor of snake venom metalloproteinases, has been completely sequenced, and its disulfide bond pattern has been experimentally determined. It shows homology to human α_1B-glycoprotein, a plasma protein of unknown function and a member of the immunoglobulin supergene family. Size exclusion and dynamic laser light scattering data indicated that two monomers of DM43, each composed of three immunoglobulin-like domains, associated to form a homodimer in solution. Analysis of its glycan moiety showed the presence of *N*-acetylglucosamine, mannose, galactose, and sialic acid, most probably forming four biantennary *N*-linked chains. DM43 inhibited the fibrinogenolytic activities of bothrolysin and jararhagin and formed 1:1 stoichiometric stable complexes with both metalloproteinases. DM43 was ineffective against atrolysin C or A. No complex formation was detected between DM43 and jararhagin C, indicating the essential role of the metalloproteinase domain for interaction. Homology modeling based on the crystal structure of a killer cell inhibitory receptor suggested the existence of an I-type Ig fold, a hydrophobic dimerization surface and six surface loops potentially forming the metalloproteinase-binding surface on DM43.

The natural resistance to envenomation by snakes observed in a few warm-blooded animals as well as in several snakes can be explained, in most cases, by the presence of soluble proteins in the resistant animals' sera, which can be grouped as inhibitors of either phospholipase A_2 (antimyotoxic and antineurotoxic factors) or snake venom metalloproteinases (SVMPs[1]; antihemorrhagic factors) (for reviews, see Refs. 1–4).

SVMPs are typically found in venom of Viperidae snakes (5). They are classified as members of the reprolysin subfamily of metalloproteinases (6), which also includes ADAMs, proteins composed of a disintegrin and metalloproteinase domain, which function in various physiological processes such as fertilization, cytokine shedding, and neurogenesis (7). SVMPs and ADAMs present many similar structural features as evidenced by their sequence and domain homologies (8). The reprolysins share with matrix metalloproteinases a conserved overall topology, a zinc-binding consensus motif, and a strictly conserved methionine near their active sites. For these reasons, SVMPs, ADAMs, and matrix metalloproteinases have been classified together as the metzincins (6, 9).

Some SVMPs induce local hemorrhage apparently as a primary consequence of the degradation of extracellular matrix proteins, although their exact mechanism of action is still unclear (10–12). Several SVMPs have been sequenced and/or cloned, and five crystal structures are available (13–17). SVMPs are organized into four classes (P-I to P-IV) according to their domain structure. The P-I class presents only the metalloproteinase domain. The P-II members have a disintegrin domain carboxyl-terminal to the proteinase domain. The P-III class has a disintegrin-like domain and a cysteine-rich domain following the proteinase domain. The P-IV class has, in addition to the previously described domains, a lectin-like domain carboxyl-terminal to the cysteine-rich domain. All classes share a homologous signal, latency, and metalloproteinase domain structure in their zymogen form (18, 19).

Less is known about the structural characteristics of the natural inhibitors of SVMPs isolated from the sera of resistant animals. Most of them are acidic glycoproteins with molecular masses varying from 52 to 90 kDa. They inhibit the enzymatic activity of hemorrhagic SVMPs through noncovalent complex formation, but are not effective against venom serine proteinases or non-venom proteolytic enzymes (20, 21). The serum antihemorrhagins most thoroughly studied are as follows: 1) Habu serum factor from the Japanese Habu snake *Trimeresurus flavoviridis* (22) and BJ46a from *Bothrops jararaca* (23), members of the superfamily of cystatins; and 2) the inhibitors isolated from the North American opossum *Didelphis virginiana* (oprin) (24) and from the mongoose *Herpestes edwardsii* (antihemorrhagic factor 1–3) (25, 26), members of the immunoglobulin supergene family. Both Habu serum factor and

* This work was supported by grants from the Conselho Nacional de Desenvolvimento Cientifico e Tecnológico, the Coordenação de Aperfeiçoamento de Pessoal de Nível Superior, the Fundação de Amparo à Pesquisa do Estado do Rio de Janeiro, the Financiadora de Estudos e Projetos, the Fundação de Amparo à Pesquisa do Estado de São Paulo, the Universidade Federal do Rio de Janeiro, the Fundação Univérsitária José Bonifacio, and the Programa de Apoio à Pesquisa Estratégica em Saúde-Fiocruz and by National Institutes of Health Grant GM57908 (to J. W. F.). The costs of publication of this article were defrayed in part by the payment of page charges. This article must therefore be hereby marked "*advertisement*" in accordance with 18 U.S.C. Section 1734 solely to indicate this fact.

The amino acid sequence reported in this paper has been submitted to the Swiss Protein Database under Swiss-Prot accession number P82957.

** To whom correspondence should be addressed. Tel.: 55-21-2562-7353; Fax: 55-21-2495-5765; E-mail: gilberto@iq.ufrj.br.

[1] The abbreviations used are: SVMPs, snake venom metalloproteinases; ADAM, a disintegrin and metalloproteinase; Tricine, *N*-[2-hydroxy-1,1-bis(hydroxymethyl)ethyl]glycine; RP-HPLC, reverse-phase high performance liquid chromatography; MALDI-TOF-MS, matrix-assisted laser desorption ionization time-of-flight mass spectrometry; KIR, killer cell inhibitory receptor; 2DL1, two domains and long-form number 1.

BJ46a have had their complete amino acid structures determined: the former by Edman sequencing and the latter by cloning of its cDNA. However, no member of the immunoglobulin supergene family of natural inhibitors of SVMPs has been fully sequenced.

Previously, we isolated an antihemorrhagic fraction (named the antibothropic factor) from the serum of the South American opossum *Didelphis marsupialis*. It showed antihemorrhagic, antilethal, antimyonecrotic, and antiedematogenic properties (27–30) and was active neither on snake venom serine proteinases nor on proteinases from other sources (31). Recently, two antihemorrhagic proteins, DM40 and DM43, were isolated from the antibothropic factor and characterized as SVMP inhibitors from the immunoglobulin supergene family. It was shown that these acid glycoproteins form noncovalent complexes with jararhagin, the main hemorrhagic metalloproteinase from *B. jararaca* venom (32).

In this study, the complete amino acid sequence of DM43 and its disulfide bond pattern and homodimeric quaternary structure were determined. Functional analyses in addition to molecular modeling studies were performed to better understand how this inhibitor interacts with its target metalloproteinases.

EXPERIMENTAL PROCEDURES

Materials—*N*-Isopropyliodoacetamide was from Molecular Probes, Inc. 4-Vinylpyridine was from Sigma. CNBr was from K&K Laboratories. Sequencing grade modified trypsin was from Promega; endoproteinase Asp-N was from Roche Molecular Biochemicals (Mannheim, Germany); and lysyl peptidase was from either Roche Molecular Biochemicals or Wako. All other chemicals were of analytical grade or higher quality.

DM43, Venoms, and Snake Venom Metalloproteinases—DM43 was isolated from *D. marsupialis* serum as previously described (32). Lyophilized *B. jararaca* venom was from the Army Biology Institute (Rio de Janeiro, Brazil). Jararhagin was isolated from crude venom based on the procedure of Paine *et al*. (33), except that a Superdex 200 column (1.0 × 30 cm; Amersham Biosciences, Uppsala, Sweden) equilibrated with 0.02 M Tris-HCl (pH 7.5) containing 0.02 M $CaCl_2$ and 0.15 M NaCl was used in the first purification step. Using the same methodology as for jararhagin, we were also able to purify jararhagin C and bothrolysin. Lyophilized *Crotalus atrox* venom was purchased from the Miami Serpentarium (Miami, FL). Atrolysins C and A were isolated from crude venom by previously described methods (34).

CNBr Digestion—DM43 was *S*-pyridylethylated and cleaved with CNBr as described (35). The CNBr peptides were isolated by Tricine/SDS-PAGE (36) and either digested in gel with trypsin as described below or transferred to a polyvinylidene difluoride membrane and directly N-terminally sequenced.

Lysyl Endoproteinase Digestion—DM43 alkylated with *N*-isopropyliodoacetamide (37) was digested with lysyl peptidase (1 μg/μl in 20% glycerol and 1 M Tris-HCl (pH 8.0)) without prior removal of alkylating reagents. To 200 pmol of *N*-isopropylcarboxyamidomethyl-DM43 was added 0.5 μl of enzyme solution, and this mixture was allowed to react at 37 °C for 18 h. The peptides obtained by lysyl peptidase digestion were isolated by RP-HPLC using either Zorbax (Agilent Technologies) or Jupiter (Phenomenex Inc.) C_{18} columns (2.1 × 150 mm) at 25 °C and at a flow rate of 0.2 ml/min. The absorbance was monitored at 215 nm. The solvent system used was 0.1% trifluoroacetic acid in H_2O (solvent A) and 0.09% trifluoroacetic acid in acetonitrile (solvent B). The gradient program began with 10% solvent B for 5 min and was then ramped to 45% solvent B at 50 min and to 70% solvent B at 55 min.

Endoproteinase Asp-N Digestion—A sample of *N*-isopropylcarboxyamidomethyl-DM43 was divided in two aliquots. The first half was digested with Asp-N after diluting the urea solution used during the alkylation procedure to 1 M with 0.05 M sodium phosphate (pH 8.0); the second half was desalted by RP-HPLC under the same conditions used for isolating the peptides obtained by lysyl peptidase digestion, dried by vacuum centrifugation, and dissolved in 0.05 M sodium phosphate (pH 8.0). Both aliquots were digested at an enzyme/substrate ratio of 1:200 (w/w) at 37 °C for 18 h. The peptides obtained by Asp-N digestion were purified by RP-HPLC as described above.

In-gel Tryptic Digestion—CNBr peptides isolated by Tricine/SDS-PAGE were subjected to in-gel digestion with trypsin (38), and the tryptic peptides were isolated on a Vydac C_{18} RP-HPLC column (1.0 × 150 mm; Separations Group) at 30 °C and at a flow rate of 0.05 ml/min. The absorbance was monitored at 215 nm. The solvent system used was 0.1% trifluoroacetic acid in H_2O (solvent A) and 0.09% trifluoroacetic acid in 70% acetonitrile (solvent B). The gradient program began with 15% solvent B for 10 min and was then ramped to 80% solvent B at 100 min.

Protein Sequence Analysis—N-terminal Edman sequencing of *N*-isopropylcarboxyamidomethyl-DM43 and the digestion peptides isolated by RP-HPLC or by Tricine/SDS-PAGE was performed on an Applied Biosystems Procise 494 instrument according to the manufacturers' instructions. The complete DM43 amino acid sequence was used to scan the GenBank™/EBI Data Bank and the Swiss Protein and Protein Identification Resource Databases for homologous sequences with the BLAST program (39). A directed BLAST sequence search of the Protein Data Bank (40) was used to identify candidate parent structures for homology modeling. A final alignment of all sequences of interest was automatically derived by the program MULTALIGN (41) and adjusted manually (see "Modeling Studies").

Disulfide Bridges—DM43 (57 μg, dry weight) was dissolved in 100 μl of 0.04 M Tris-HCl (pH 8.0) containing 20% acetonitrile and digested overnight at 37 °C with 1 μg of lysyl peptidase. Peptides were separated on a Zorbax 300SB C_{18} column (2.1 × 150 mm) at 32 °C and at a flow rate of 0.2 ml/min, with detection at 215 nm. The solvent system was 0.1% trifluoroacetic acid in H_2O (solvent A) and 0.09% trifluoroacetic acid in acetonitrile (solvent B). The gradient program began with 20% solvent B for 5 min and was then ramped to 55% solvent B at 50 min and to 70% solvent B at 55 min. The molecular masses of the experimentally isolated peptides were determined by MALDI-TOF-MS on a Voyager DE-PRO mass spectrometer (Perseptive Biosystems) using 3,5-dimethoxy-4-hydroxycinnamic acid as the matrix. Peptide masses were compared with theoretically possible disulfide-linked peptides and used as a guide to select peptides for Edman sequencing on the Procise 494 instrument.

Carbohydrate Content—DM43 glycan moieties were analyzed after methanolysis, followed by re-*N*-acetylation of amino sugars and trimethylsilylation of hydroxyl and carboxyl groups. The volatile trimethylsilyl derivatives were analyzed by gas chromatography-mass spectroscopy on a Shimadzu gas chromatograph using a DB-1 capillary column (0.25 mm × 30 m), and the compounds were further characterized by electron impact mass spectroscopy (42). To determine the molecular mass of the DM43 protein moiety, a sample of DM43 chemically deglycosylated by anhydrous trifluoromethanesulfonic acid (32) was analyzed by MALDI-TOF-MS as previously described.

Analysis of DM43 Quaternary Structure—The molecular mass of DM43 was determined by size exclusion chromatography under different conditions: 1) a Superdex 200 fast protein liquid chromatography column equilibrated with 0.02 M Tris-HCl (pH 7.5) containing 0.02 M $CaCl_2$ and 0.15 M NaCl; 2) the same column equilibrated with 0.05 M sodium phosphate (pH 7.0) containing 0.15 M NaCl and 6 M guanidine HCl; and 3) a Protein-Pak 300 SW HPLC column (0.78 × 30 cm; Waters) eluted with 0.1 M sodium phosphate (pH 7.0), made 0.15 M with NaCl, at a flow rate of 0.5 ml/min. Size exclusion standards (Amersham Biosciences) were bovine serum albumin (67 kDa), ovalbumin (43 kDa), and chymotrypsinogen (25 kDa). Di-bovine serum albumin (134 kDa) present in the bovine serum albumin standard was also used as a marker. Native DM43 molecular mass was also determined by dynamic laser light scattering at 20 °C using a DynaPro molecular sizing instrument (Protein Solutions, High Wicombe, United Kingdom). DM43 was dissolved in 0.05 M sodium phosphate (pH 8.0) at 2 mg/ml and filtered through a 0.02-μm membrane. Approximately 25 individual Stokes radius values were acquired for each sample and statistically averaged. Based on this averaged value and assuming a globular conformation, the molecular mass was calculated using the software provided with the instrument. The requirement of divalent ions for DM43 dimerization was assessed after its incubation with 10 mM EDTA in 0.02 M Tris-HCl (pH 7.4) containing 0.15 M NaCl for 1 or 20 h at 37 °C and analysis of the protein by size exclusion chromatography on Superdex 200 as described above.

Inhibition of SVMPs—DM43 inhibitory ability was tested against different SVMPs from the venoms of *B. jararaca* (bothrolysin, P-I, EC 3.4.24.50; and jararhagin, P-III, EC 3.4.24.73) and *C. atrox* (atrolysin C, P-I, EC 3.4.24.42; and atrolysin A, P-III, EC 3.4.24.1). To evaluate the inhibition of SVMP activity by DM43, each enzyme (0.5 μg) was incubated with fibrinogen (enzyme/substrate ratio of 1:20 (w/w)) for 10 min in either the absence or presence of DM43 at a 1:1 molar ratio. Atrolysin A (1 μg) was incubated for 6 h. The fibrinogenolytic activity of the samples was analyzed by SDS-PAGE under reducing conditions. EDTA (10 mM) was used in the incubation mixture as a control of total SVMP inhibition (32).

Complex Formation—For complex formation analysis, equimolar amounts of DM43 and each SVMP were incubated for 10 min at 37 °C in 0.02 M Tris-HCl (pH 7.5) containing 0.02 M $CaCl_2$ and 0.15 M NaCl. In one set of experiments, equimolar amounts of jararhagin and DM43 were incubated for 30 min at 37 °C in the presence of 10 mM EDTA in 0.02 M Tris-HCl (pH 7.4) containing 0.15 M NaCl. Samples were chromatographed at 0.5 ml/min on a Superdex 200 column equilibrated with the incubation buffer. The various eluted fractions were collected, precipitated with 10% trichloroacetic acid (final concentration), and analyzed by SDS-PAGE under (non)reducing conditions. Jararhagin C, a disintegrin-like/cysteine-rich domain protein resulting from proteolytic processing of jararhagin from *B. jararaca* venom (43), was also tested for complex formation with DM43 using the above conditions. To check for dissociation, the DM43-jararhagin complex was isolated by Superdex 200 as described above, incubated with a 2-fold molar excess of bovine fibrinogen for 5 min at 37 °C, and reinjected onto the Superdex column. Finally, to evaluate whether DM43 forms a complex with jararhagin under "physiological conditions" (in the venom), crude *B. jararaca* venom and DM43 were incubated in phosphate-buffered saline at a 10:1 (w/w) ratio for 15 min at 37 °C and then analyzed by native PAGE (31). Proteins were either stained with Coomassie Blue or immunoblotted using anti-DM43 polyclonal antibodies as described by Neves-Ferreira *et al.* (31).

Stoichiometry of the DM43-Jararhagin Complex—A fixed amount of jararhagin was incubated with DM43 at different molar ratios (jararhagin/DM43 at 1:0.4 to 1:4.8). Protein contents were determined using molar coefficients at 280 nm for DM43 (60,305 M^{-1} cm^{-1}) and jararhagin (54,385 M^{-1} cm^{-1}) determined as described (44). Each sample was analyzed by size exclusion chromatography on Superdex 200 in Tris-HCl buffer as described previously. Jararhagin and DM43 controls were individually submitted to the same experimental procedure. The samples were collected, precipitated with 10% trichloroacetic acid (final concentration), and analyzed by SDS-PAGE. The molecular mass of the DM43-jararhagin complex was calculated by size exclusion chromatography as well as by dynamic laser light scattering as already described for DM43 alone.

Modeling Studies—A specific BLAST sequence search of the Protein Data Bank (40) using default parameters was used to identify candidate parent structures for homology modeling. The first of the Ig-like domains of DM43, here denominated D0, was built on the D2 domain of the natural killer cell inhibitory receptor KIR2DL1 (Protein Data Bank code 1nkr) (45), whereas the second and third domains (D1 and D2) were built concomitantly on the corresponding domains of the same parent structure (see Fig. 2). Models were constructed with the automated homology modeling program MODELLER 4 (46). The initial input alignment was automatically derived from the program MULTALIGN of the AMPS suite (41) using the PAM250 matrix and a gap penalty of 8 prior to manual adjustment. The low sequence identity between the DM43 Ig domains and those of KIR2DL1 led to ambiguities in the alignment, requiring the construction of several alternative models (over 200 in total) in which slight modifications to the alignment were made. Typically, 10 models were built for each alignment using a protocol that involved coordinate copying for atoms in common with code 1nkr and using internal coordinates from the CHARM topology library (47) for the remainder. A 4-Å coordinate randomization was applied to each structure prior to optimization using up to 300 cycles of the variable target function method employing conjugate gradients. Refinement was subsequently performed in Cartesian space using the standard full molecular dynamics algorithm with simulated annealing as implemented in MODELLER 4. Distance restraints were applied up to 14 Å in the case of C-α–C-α distances and 11 Å for N–O distances. Additional restraints were applied to the hydrogen bonds involving the O-γ atoms of the serines of the WS*X*WS box and to fix the C and C′ strands of the I-type Ig fold. The deviation permitted for the proline ϕ angle was also further restricted to avoid disallowed regions of Ramachandran space.

The quality of the models generated was evaluated by reference to the MODELLER pseudo-energy term as well as by use of the structure verification programs PROCHECK (48) and VERIFY_3D (49) and the QUALITY option (50) of WHATIF (51). Potential interface regions on the surface of the models were analyzed with the program PATCHES (52) using default parameters for dimeric contacts.

RESULTS

Primary Structure, Disulfide Bridges, and Carbohydrate Content of DM43—The strategy used to elucidate the primary structure of DM43 was the N-terminal sequencing of the intact protein and the determination of the amino acid sequences of a set of peptides generated by cleavage at peptide bonds adjacent to methionine, lysine, aspartic acid or arginine, and lysine. A summary of the DM43 complete amino acid sequence is shown in Fig. 1, along with all peptides and overlaps necessary for the proof of the sequence. This SVMP inhibitor was found to be composed of 291 amino acid residues. Cycles corresponding to positions 23, 156, 160, and 175 produced no detectable phenylthiohydantoin-derivatives and could be identified as the first position of *N*-glycosylation consensus sequences. Analysis of the DM43 glycan part indicated the presence of *N*-acetylglucosamine, mannose, galactose, and sialic acid at 4:3:2:2 molar ratios. After chemical deglycosylation, the molecular mass of the DM43 protein moiety, as determined by MALDI-TOF-MS, was 33,651.6 Da (Table I). Compared with the previously determined mean molecular mass for native DM43 (42,691 Da) (32), one can assume a molecular mass of 9039 Da for its glycan moiety, which represents 21% of the total molecular mass of DM43. The disulfide bond pattern of DM43 was determined using a combination of MALDI-TOF-MS and Edman sequencing of peptides isolated by RP-HPLC after lysyl peptidase digestion. The second bridge (Cys^{121}–Cys^{163}) was clearly established after parallel sequencing the disulfide-linked peptides ^{119}LH***X***RGMLLGMIFDLYQEGEQEP^{140} and ^{143}SSQTPSAEATFIV***X***STG***X***YS***X***LYRAPASAPSV^{174}. The third bond (Cys^{213}–Cys^{265}) was also unambiguously determined after sequencing the linked peptides ^{193}ANFYILNDRDFRPGDIVTFS***X***WARFSEREYDLEFK^{227} and ^{263}YS***X***RYRFRNGPPIWSEDSNVLELDLSTG^{290}. A peptide containing only the expected parallel sequences ^{14}TESPS . . . Cys^{28} . . . FQVWK^{42} linked to ^{59}FWLGP . . . Cys^{74} . . . EVTGK^{95} was not seen.

DM43 amino acid sequence showed homology to α_1B-glycoprotein, a human plasma protein of unknown function and a member of the immunoglobulin supergene family (53). In a 271-residue overlap, 101 residues (37%) were found to be identical, and 39 residues (14%) were conservative substitutions, giving 51% overall similarity. DM43 was also homologous to

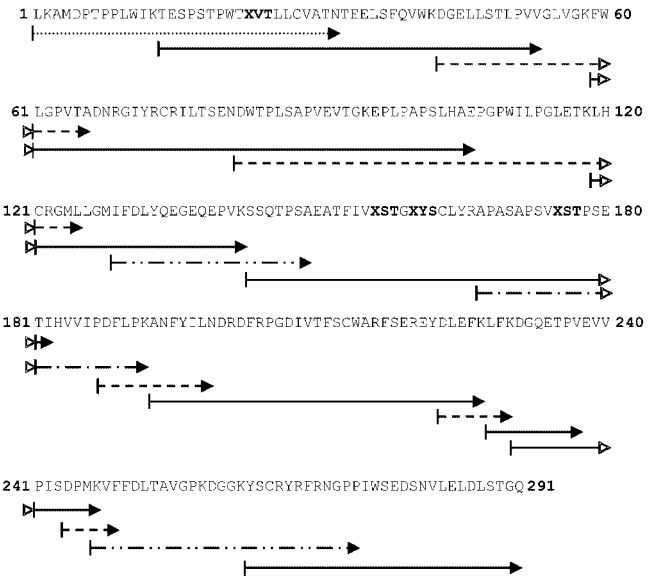

FIG. 1. **Summary of the complete amino acid sequence of DM43.** A minimum set of overlapping peptides was used to determine the sequence. Direct N-terminal sequence of *N*-isopropylcarboxyamidomethyl-DM43 gave the first 32 residues (····). The peptides obtained from different digestions are as follows: lysyl peptidase peptides (——), endoproteinase Asp-N peptides (– – –), CNBr fragments (– · · –), and tryptic peptide of a CNBr fragment (– · – ·). The four putative *N*-linked glycosylation sites are in *boldface*. *Closed arrows* indicate the end of a peptide. *Open arrows* indicate that the sequence continues in the next line until the next *closed arrow*.

TABLE I
Molecular masses of DM43, jararhagin, and the DM43-jararhagin complex determined by different methods

	Molecular mass as determined by:			
	SDS-PAGE	MS[a]	Size exclusion	DLLS
	kDa	*Da*	*kDa*	*kDa*
DM43	47[b]	42,691[b]	73	78
DM43 in guanidine HCl	ND	ND	42	ND
Deglycosylated DM43	34[b]	33,652	ND	ND
DM43 + jararhagin	ND	ND	104	100
Jararhagin	52[c]	46,073[d]	54	ND

[a] MS, mass spectrometry; DLLS, dynamic laser light scattering; ND, not determined.
[b] Ref. 32.
[c] Ref. 33.
[d] Determined by electrospray ionization.

two partially sequenced SVMP serum inhibitors: oprin from the opossum *D. virginiana* (24) (86% identity over 237 residues) and AHF-1 from the mongoose *H. edwardsii* (26) (44% identity over 124 residues). More limited sequence identity was also detected in the Ig-like domains of KIR2 and KIR3 molecules, membrane-bound receptors that are found on natural killer cells and that specifically detect the presence of class I human leukocyte antigen molecules on host cells (54). An alignment of all relevant sequences, including those used as the basis for homology modeling, is shown in Fig. 2.

Analysis of DM43 Quaternary Structure and Functional Studies—The molecular mass of native DM43 was determined by size exclusion chromatography (73 kDa) and dynamic laser light scattering (78 kDa). Incubation of DM43 with EDTA did not modify the elution volume of native DM43 on Superdex 200. Size exclusion chromatography under denaturing conditions yielded 42 kDa, in agreement with the mass spectrometry result. Taken all together, these molecular mass values indicate a homodimeric structure for DM43 (Table I).

DM43 completely inhibited the proteolytic activity of bothrolysin or jararhagin against fibrinogen at a 1:1 molar ratio (Fig. 3). Nonetheless, no inhibition of atrolysin A and only poor inhibition of atrolysin C fibrinogenolytic activities were seen when a 4-fold molar excess of DM43 was used (data not shown). As shown in Fig. 4, DM43 formed a stable noncovalent complex with bothrolysin. Confirming previous results (32), DM43 complexed with jararhagin, either isolated or within the crude venom (Fig. 5), but the complex was not dissociated in the presence of a molar excess of fibrinogen (data not shown). When jararhagin was incubated with EDTA, its elution behavior on Superdex 200 changed quite drastically, probably as a consequence of a loss of conformation. Jararhagin (usually eluted at 14 ml as a single peak) eluted as two peaks at 11.3 and 12.2 ml. Under this condition, no complex formation with DM43 was observed. No proteolysis of either inhibitor or SVMPs was observed following the incubation of DM43 with bothrolysin (Fig. 4) or jararhagin (32) and analysis by SDS-PAGE under (non)reducing conditions. The titration assay to determine the stoichiometry of the complex between jararhagin and DM43 indicated interaction of one molecule of the hemorrhagin with one monomer of DM43 (Fig. 6). At this molar ratio, almost no free jararhagin or DM43 was observed, and there was a clear saturable amount of complex formed. Moreover, the molecular masses of the complex, as determined by size exclusion chromatography (104 kDa) and dynamic laser light scattering (100 kDa) (Table I), supported the hypothesis that DM43 interacts as a monomer with one molecule of jararhagin. Interestingly, DM43 did not form complex with jararhagin C (data not shown), a fragment of jararhagin lacking the metalloproteinase domain. Also, one could not detect any interaction between DM43 and atrolysin C or A by size exclusion chromatography.

Model Structure of DM43—Protein Data Bank code 1nkr, corresponding to the extracellular region of the KIR2DL1 natural killer cell inhibitory receptor, was chosen as the parent structure for the models of both the D1/D2 domains of DM43 and D0, in preference to alternative homologs, because of its superior resolution, *R*-factor, and stereochemical parameters. The overall sequence identity between the D1/D2 domains and the equivalent domains from KIR2DL1 was 27.7%, and that between the D0 and D2 domains of KIR2DL1 was 28.1%. The final alignment used in the construction of the models is shown in Fig. 2.

The models generated by the MODELLER program were subjected to local manual adjustments using the interactive modeling program WHATIF. The overall residual pseudo-energy of the D1/D2 model after manual adjustment, given by $-\ln(P)$, where P is the molecular probability density function defined by MODELLER, was 1982.8, which is comparable to that of the starting structure (1684.7); that of the D0 model was 515.37, compared with 826.72 (46). The stereochemistry of the models, as measured by the PROCHECK *G*-factors, was acceptable in both cases: −0.39 for D0 and 0.27 for D1/D2, equivalent to crystal structures of 2.0- and <1.0-Å resolution, respectively (48). The models for D1/D2 and D0 present only two and five residues, respectively, in the "generously" allowed regions of the Ramachandran plot and no residue within the disallowed regions (55). However, the overall quality of the structure is probably better determined by parameters that assess residue environments and atomic contacts. The VERIFY_3D scores for D0 and D1/D2 were 25.81 and 59.77, respectively, well above the threshold for correct structures (19.13 and 38.88, respectively, for proteins of equivalent lengths) (49). The WHATIF quality scores were also satisfactory: −1.34 and −0.93 for D0 and D1/D2, respectively, corresponding to "good or very good modeled structures" according to the classification of Vriend and Sander (50).

Fig. 7 shows ribbon diagrams for DM43 final homology-built models. All three domains present a type-I Ig fold (56) in which the A strand is divided between the two β-sheets due to a bulge caused by a *cis*-peptide bond. In the D1 domain, this *cis*-peptide is readily accommodated by Pro^{107}, but its authenticity in the remaining domains of DM43 is questionable. One of the most notable features of the DM43 amino acid sequence is the presence of a degenerate WS*X*WS box (57) in each domain. This sequence motif is situated between the F and G strands of the Ig fold and was first described in the hematopoietic receptor family. It has subsequently also been observed in KIRs (45). Its most conserved features are the two serine residues whose side chain hydroxyl groups donate hydrogen bonds to the backbone amides of a neighboring β-strand. The most authentic of the WS*X*WS box motifs present in DM43 is observed in the D2 domain and is highlighted in Fig. 7. As observed in KIR2 structures, the first tryptophan of the motif (Trp^{276}) is sandwiched between the D1 and D2 domains and, together with a cluster of hydrophobic residues (including Trp^{110}, Val^{185}, Pro^{187}, Phe^{229}, and Pro^{236}) and a series of interdomain hydrogen bonds provided by an F′ strand in D2, appears to be an important component of this interface. These contacts are presumably responsible for stabilizing the acute elbow angle of ~60° between D1 and D2. This relative domain organization is typical of KIRs and hematopoietic receptors (58, 59), but rather different from that seen in immunoglobulins, which generally present a much more open elbow angle. The relative orientation of the D0 and D1 domains is less easily predicted. However, an acute elbow angle would not be expected in this case,

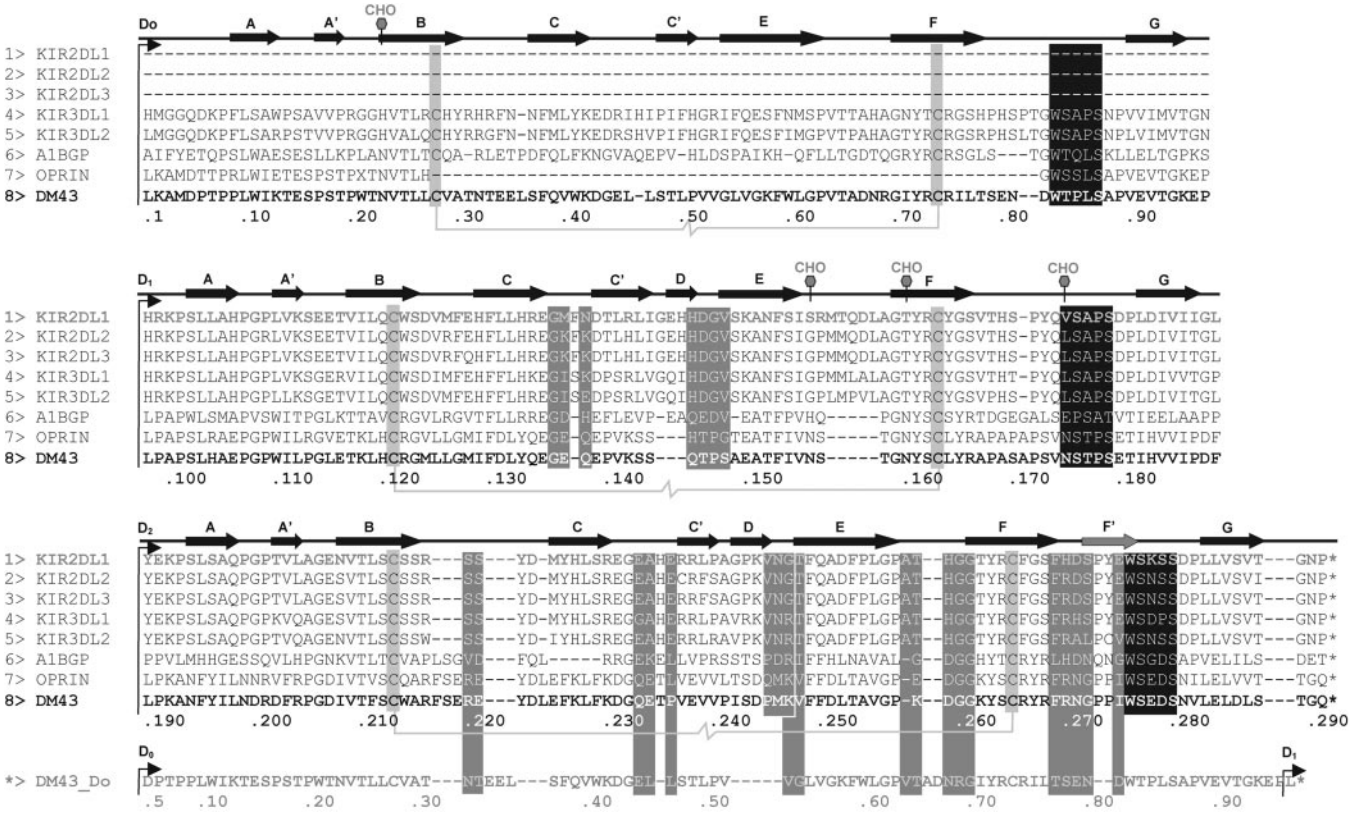

FIG. 2. **Comparison of the amino acid sequences of DM43, oprin, KIRs, and α_1B-glycoprotein**. The final alignment was performed by the MULTALIGN program prior to manual adjustment. KIR2DL and KIR3DL refer to distinct KIR2 and KIR3 natural killer inhibitory receptor sequences, and A1BGP refers to the first three domains of human α_1B-glycoprotein. Oprin and DM43 refer to the metalloproteinase inhibitors from *D. virginiana* and *D. marsupialis*, respectively. DM43 glycosylation sites (*CHO*) are indicated. *Horizontal arrows* indicate the β-strands of the Ig fold as assigned by the PROMOTIF program (70) to Protein Data Bank code 1nkr, corresponding to KIR2DL1. Ig-like domains are limited by *vertical bent arrows*, and the WS*X*WS motif is *boxed* (*black*). Also shown in boxes (*gray*) are the half-cystine residues that form the internal disulfide bridge of each domain and regions of the sequence alignment that were deliberately misaligned during model construction.

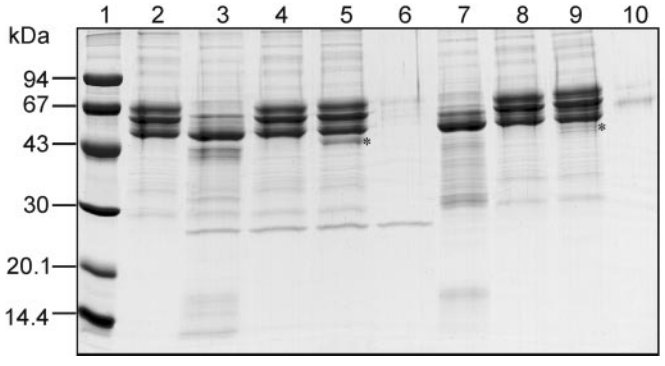

FIG. 3. **Inhibition of bothrolysin and jararhagin fibrinogenolytic activities by equimolar amounts of DM43.** *Lane 1*, molecular mass markers; *lane 2*, fibrinogen control; *lane 3*, fibrinogen + bothrolysin; *lane 4*, fibrinogen + bothrolysin/EDTA; *lane 5*, fibrinogen + bothrolysin/DM43; *lane 6*, bothrolysin; *lane 7*, fibrinogen + jararhagin; *lane 8*, fibrinogen + jararhagin/EDTA; *lane 9*, fibrinogen + jararhagin/DM43; *lane 10*, jararhagin. The position of DM43 on the gel is indicated (*). Samples were analyzed by 12% SDS-PAGE and stained with Coomassie Blue.

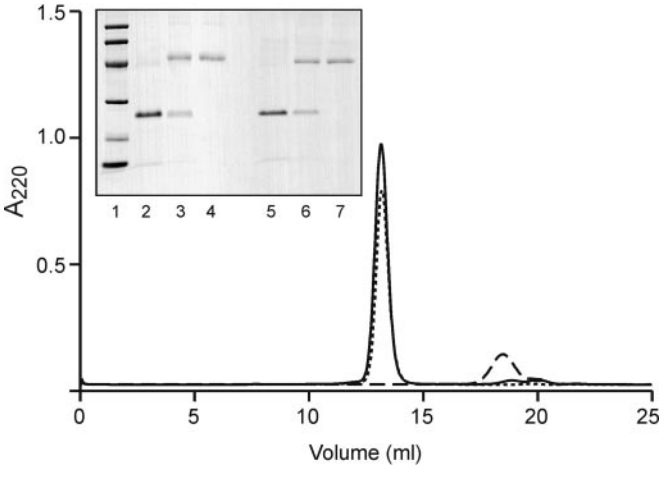

FIG. 4. **Complex formation between DM43 and bothrolysin**. Samples were analyzed by size exclusion chromatography on Superdex 200. – – –, bothrolysin; · · · ·, DM43; ——, bothrolysin + DM43. *Inset*, Coomassie Blue-stained 12% SDS-polyacrylamide gel of the above chromatography samples. *Lane 1*, molecular mass markers (see Fig. 3); *lanes 2* and *5*, bothrolysin without and with β-mercaptoethanol, respectively; *lanes 3* and *6*, complex without and with β-mercaptoethanol, respectively; *lanes 4* and *7*, DM43 without and with β-mercaptoethanol, respectively.

as the WS*X*WS motif in D1 lacks the relevant tryptophan. Furthermore, it is substituted by a glycosylated asparagine, whose carbohydrate moiety would sterically prevent close approximation of the two domains.

DISCUSSION

Most, if not all, Viperidae venoms contain SVMPs, many of which play an important role in the pathogenesis of local tissue alterations. In severe envenomations, SVMPs can cause bleeding in organs distant from the site of the bite, such as heart, lungs, kidneys, and brain (10, 60). There is a growing interest in studying inhibitors of SVMPs such as DM43. Of significance is the possibility that these inhibitors could be used as therapeutic alternatives for the treatment of snake envenomation. Moreover,

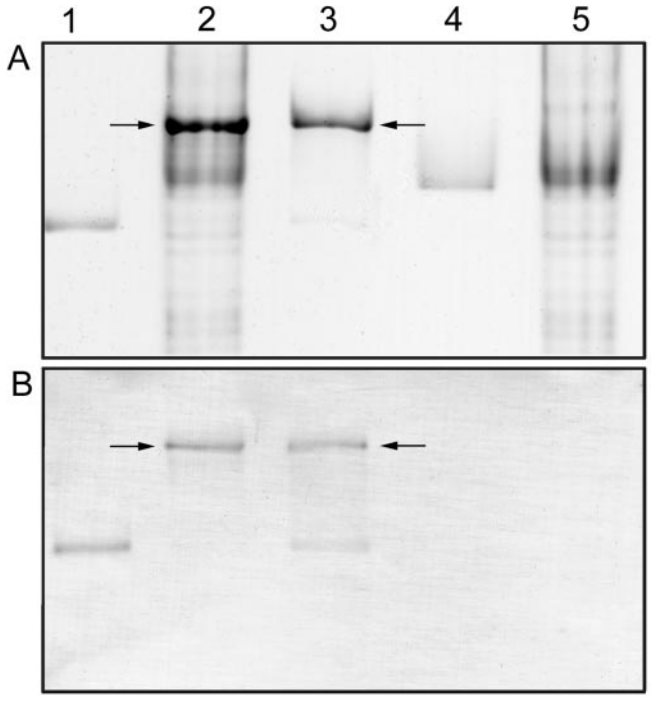

FIG. 5. **PAGE (12%) analysis of complex formation between DM43 and jararhagin in venom**. *A*, Coomassie Blue staining; *B*, Western blotting developed with polyclonal antibodies raised against DM43. *Lane 1*, DM43; *lane 2*, DM43 + *B. jararaca* venom (1:10, w/w); *lane 3*, DM43 + jararhagin (1:1 mol/mol); *lane 4*, jararhagin; *lane 5*, *B. jararaca* venom. *Arrows* indicate the position of the complex on the gel.

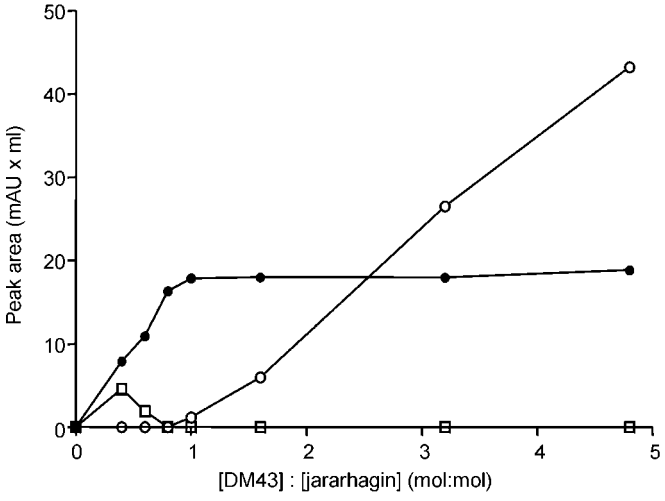

FIG. 6. **Titration of jararhagin by DM43.** A fixed amount of jararhagin was mixed with increasing amounts of DM43, and the samples were submitted to size exclusion chromatography on Superdex 200. At each molar ratio, peak areas corresponding to free DM43 (○) or jararhagin (□) and to the DM43-jararhagin complex (●) were integrated and plotted. *mAU*, milli-absorbance units.

SVMPs have been shown to have several structural features similar to the recently discovered ADAMs, proteins containing disintegrin and metalloproteinase domains that are potentially involved in both cell adhesion and protease activities (7, 8, 61). Thus, the study of their inhibition mechanism could also improve our understanding of ADAM function. Interestingly, although tissue inhibitor of matrix metalloproteinase-3 was shown to be a good inhibitor of ADAM-17 (62), ADAM-10 (63), ADAM-12-S (64), and ADAM-TS4 and ADAM-TS5 (65), no ADAM-specific inhibitor has been described thus far.

The closest homologs to the SVMP inhibitor DM43 are the antihemorrhagins isolated from the North American opossum *D. virginiana* (oprin) (24) and the single chain α_1B-glycoprotein isolated from human plasma (53). DM43 possesses three Ig-like domains homologous to those found in the N-terminal region of α_1B-glycoprotein, a five-domain protein. Somewhat more distant relatives are the extracellular portions of the natural killer cell inhibitory receptor KIR2 and KIR3 molecules, which possess two and three Ig-like domains, respectively (54). Crystal structures have been reported only for KIR2 (45, 66, 67). Human natural killer cells are a class of lymphocytes that kill certain virus-infected or tumor cells and are involved in innate immunity against viruses, intracellular bacteria, and parasites. The inhibitory signal generated in response to the absence of the major histocompatibility complex class I molecules on the target cell surface is the default command that indicates that the target is abnormal and should be lysed by the natural killer cell (54).

Each of the three domains of DM43 possesses two cysteine residues, which form the classical intersheet disulfide bridge linking β-strands B and F of the Ig fold. The aromatic residue that is generally observed to pack over the bridge and that originates from β-strand C is also conserved in all three domains. The disulfide bridges linking Cys^{121} and Cys^{163} and Cys^{213} and Cys^{265} in the second and third DM43 domains, respectively, were experimentally confirmed. Considering the absence of free thiol groups in this protein (32), the existence of a disulfide bridge linking Cys^{28} and Cys^{74} in the first DM43 Ig-like domain can be inferred.

These signature residues of the Ig fold are probably important to its stability and are also present in the corresponding domains of the α_1B-glycoprotein. These data confirm the expected disulfide bond pattern for a protein of the immunoglobulin supergene family and reinforce the validity of our structural model. All of these multidomain members of the immunoglobulin supergene family have presumably arisen by gene duplication of a primordial gene coding for a single domain of ~95 amino acid residues (68).

The putative glycosylation sites of DM43 and oprin (at positions 23 and 160) align with two of the four glucosamine attachment sites in α_1B-glycoprotein. Positions 156 and 175, which also gave no detectable phenylthiohydantoin-derivatives, are *N*-glycosylated in oprin (24) and could represent additional carbohydrate linkages in DM43. All these putative glycosylation sites were found in *N*-glycosylation consensus sequences N*X*T and N*X*S (*X* ≠ Pro) (Fig. 1). Considering the presence of four biantennary *N*-linked chains (each one composed of four *N*-acetylglucosamines, three mannoses, two galactoses, and two sialic acids) and using average molecular masses for these carbohydrates, one would expect a theoretical molecular mass of 8816 Da for the glycan moieties of DM43, in close agreement with the experimentally determined value of 9039 Da.

The molecular mass values obtained for native DM43 by size exclusion chromatography (73 kDa) and dynamic laser light scattering (78 kDa) are in contrast with the masses determined by SDS-PAGE (47 kDa), MALDI-TOF-MS (42,691 Da), and size exclusion chromatography under denaturing conditions (42 kDa) (Table I), indicating a dimeric structure in solution, which is apparently not dependent on the presence of divalent ions such as Ca^{2+}. This is the first time that evidence of a nonmonomeric nature for the low molecular mass antihemorrhagins of the immunoglobulin supergene family has been presented.

DM43 inhibited the proteolytic activities of bothrolysin and jararhagin on fibrinogen and formed stable noncovalent complexes with both of them, although no complex formation was observed when jararhagin was incubated with DM43 in the

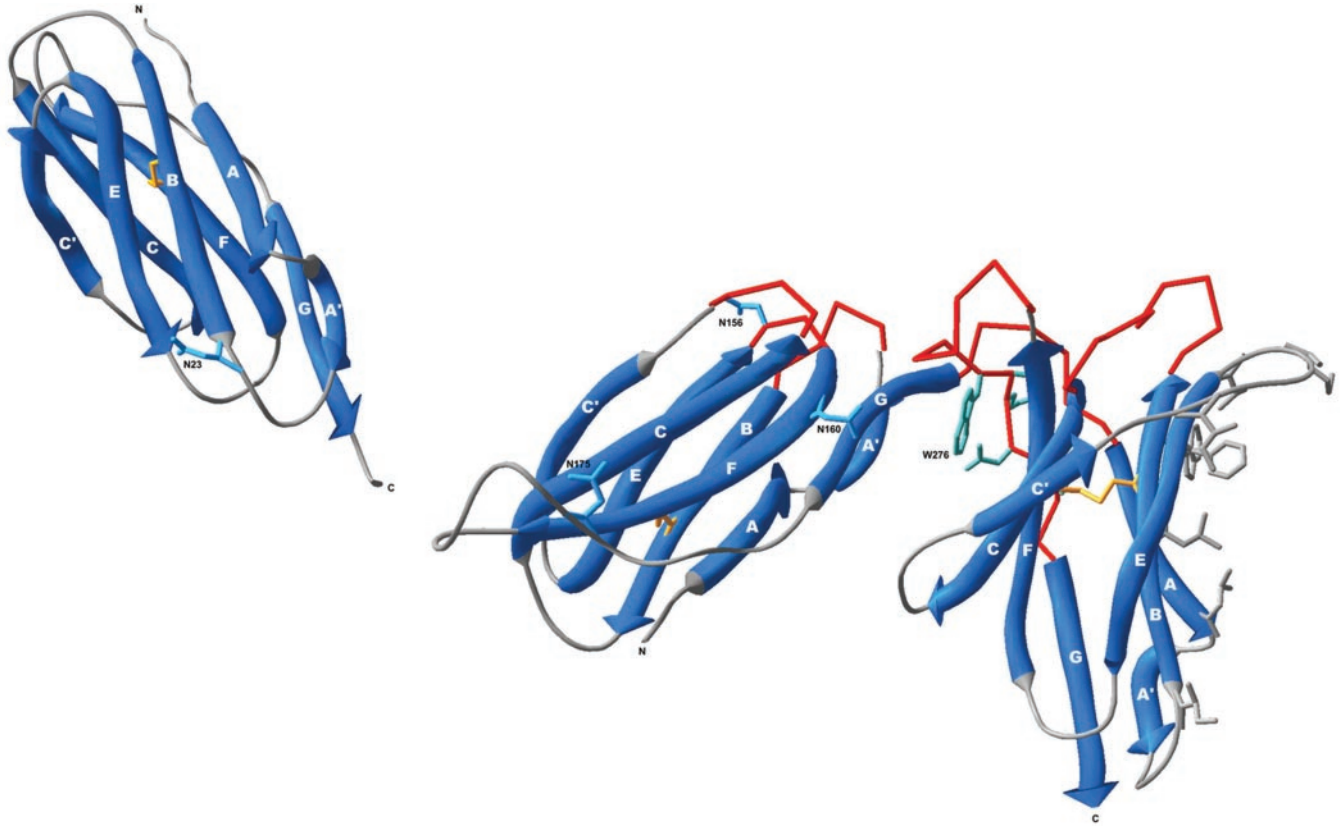

FIG. 7. **Ribbon model of the three-dimensional structure of DM43.** D0 is shown separately on the left, D1 in the center, and D2 to the right. The asparagine side chains corresponding to the four solvent-exposed glycosylation sites present on D0 and D1 are shown in *pale blue*, as are the side chains of the WS*X*WS box motif of D2 (including Trp^{276} at the interface between D1 and D2). Disulfide bridges are shown in *yellow*. The hydrophobic patch of residues arising largely from the B and E strands of D2 is shown in *gray* to the right and is believed to form the homodimerization interface. The six loops on D1/D2 that are predicted to form the metalloproteinase recognition surface are highlighted in *red*.

presence of EDTA. This last result is somewhat expected given the well known dependence of SVMPs on metal ions such as Zn^{2+} and Ca^{2+} for catalysis and conformational stabilization, respectively (69). We also showed that DM43 is able to form complexes not only with isolated jararhagin, but also with this SVMP in whole venom. This suggests that inhibition of the toxicity of the SVMPs could be one of the physiological functions of DM43. Corroborating this hypothesis is the fact that fibrinogen, a physiological substrate for jararhagin, does not induce the dissociation of the DM43-jararhagin complex. On the other hand, DM43 was not effective against atrolysin C or A. The reason for the inhibition of *B. jararaca* SVMPs in contrast to the lack of inhibition of atrolysins from *C. atrox*, despite the high level of sequence similarity among these reprolysins, is unclear (see below). Oprin, a DM43 homolog isolated from *D. virginiana* opossum serum, was also not effective against atrolysin A and only partially inhibited the hemorrhagic activity of *C. atrox* venom (24). The presence of a second inhibitor in opossum serum that would be responsible for atrolysin A inhibition observed with crude serum was suggested. Recently, we isolated a second inhibitor from *D. marsupialis* serum (DM40) (32), and its inhibitory specificity for different SVMPs is under investigation.

As already seen, DM43 has a homodimeric structure as isolated from the serum. The titration assay indicated that when DM43 was saturated with the SVMP jararhagin, there was an end complex of one subunit of inhibitor and one proteinase molecule. On the other hand, no complex formation was detected between DM43 and jararhagin C, which points to the essential role of the metalloproteinase domain. Moreover, DM43 was also able to form a complex with bothrolysin, a P-I SVMP, indicating that the metalloproteinase domain alone can be responsible for the interaction. Fractionation of the complex by SDS-PAGE, with and without reduction, indicated that no covalent bond was formed between the enzyme and the inhibitor and that the latter was not cleaved by the enzyme.

The modeled structure of DM43 shows that the acute elbow angle between D1 and D2 brings together six exposed loops on the convex surface formed by these domains (Fig. 7). By analogy with hematopoietic receptors, specifically the growth hormone (58) and prolactin (59) receptors, for which crystal structures of ligand-receptor complexes are known, these loops are expected to form the binding surface for the ligand. In the case of DM43, this region is therefore predicted to form the venom metalloproteinase recognition site. On the basis of this assumption, the model for D1/D2 allows the testable prediction that residues within the loops connecting β-strands A′ to B, C to C, and E to F of the D1 domain and those connecting β-strands B to C and F to G of the D2 domain, together with the interdomain linker, will be responsible for ligand binding in DM43. More specifically, these regions correspond to residues 113–116, 136–138, 156–158, 188–193, 216–224, and 270–282, respectively.

This predicted binding surface bares an overall negative charge, which may provide insight into the specificity of SVMP recognition by DM43. Both atrolysins A (18) and C (14), which at most interact only weakly with DM43, possess a highly negatively charged loop (including the sequence DEE) at the entrance to the cleft leading to the metalloproteinase active site. This may be expected to disfavor binding. On the other hand, the equivalent residues in jararhagin (NGP) (33) are uncharged, which may explain higher affinity via a reduction in electrostatic repulsion.

Analysis of the molecular surface of the models showed the

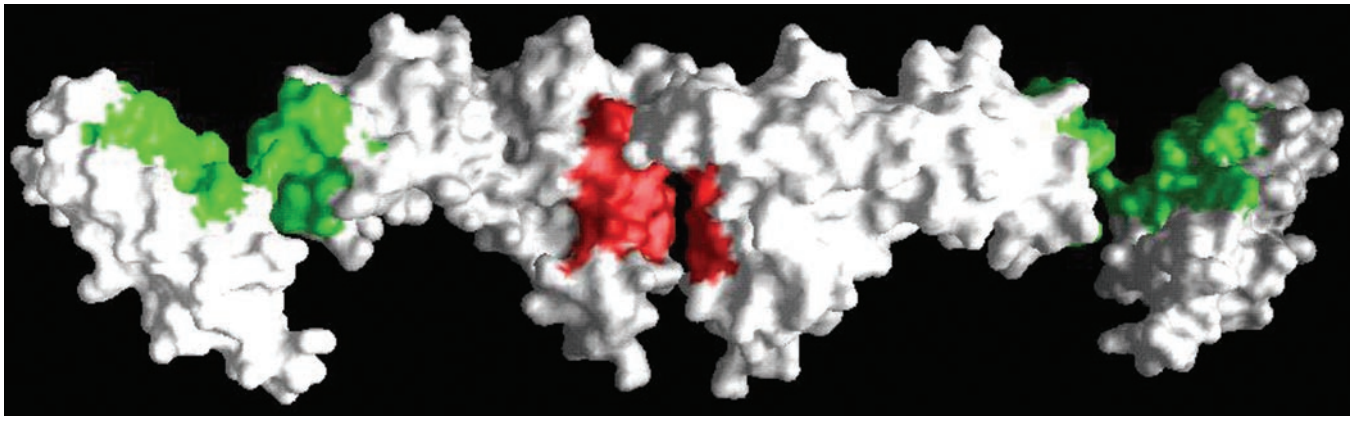

FIG. 8. **Analysis of potential interface regions on DM43 with the PATCHES program.** The patches identified on D0 and D1 (shown in *green*) probably correspond to the contact region between these domains. The large patch on D2 (shown in *red*) corresponds to a cluster of hydrophobic residues probably responsible for the formation of DM43 homodimers in solution.

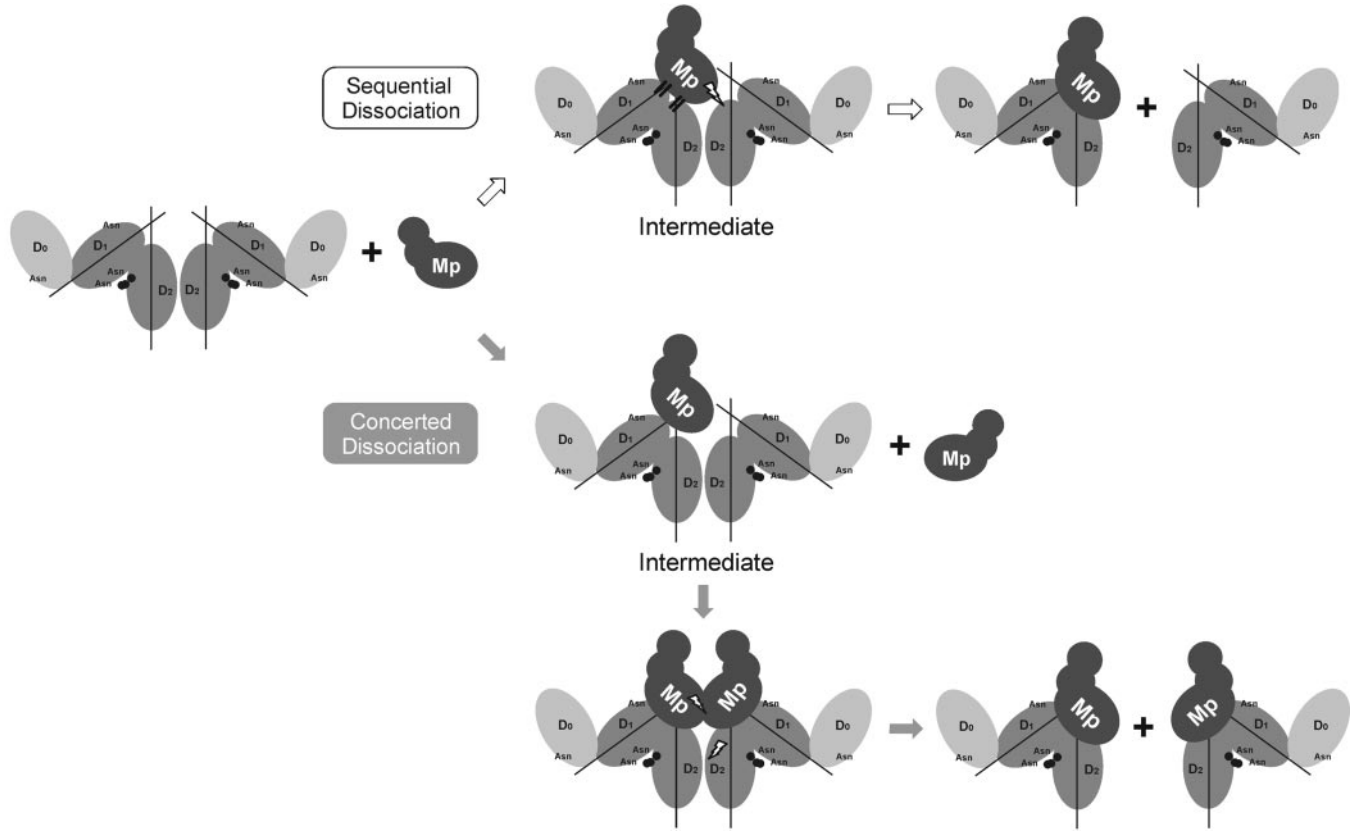

FIG. 9. **Hypothetical mechanism of interaction between SVMPs and DM43.** Given that the stoichiometry of the final complex between DM43 and SVMP is 1:1 and that the DM43 homodimer dissociates during complex formation, two generic mechanisms are presented for which we coined the terms concerted and sequential dissociation. The *lightning bolts* represent regions of potential steric hindrance that may lead to dissociation of the DM43 homodimer. *Mp*, metalloproteinase.

presence of exposed hydrophobic clusters on all three domains. These regions were confirmed with the PATCHES program (52), which is designed to identify potential interface regions on monomers derived from oligomeric complexes. The patches identified on D0 and D1 (shown in *green* in Fig. 8) probably correspond approximately to the contact region between these domains. The large patch on D2, shown in *red* (Fig. 8), corresponds to a cluster of hydrophobic residues located principally on β-strands B and E. We suggest that this region corresponds to the interface responsible for the formation of homodimers of DM43 in solution.

Given that the final complex between DM43 and SVMP presents a 1:1 stoichiometry, it is necessary for the DM43 homodimer to dissociate during complex formation. The observations made above allow us to propose a hypothetical mechanism for such dissociation in which the ligand-binding loops from one or both of the DM43 monomers initially interact with the metalloproteinase (Fig. 9). Two generic mechanisms are presented for which we coined the terms concerted and sequential dissociation. In the concerted dissociation mechanism, intermediates with 2:1 and 2:2 stoichiometries are formed along the mechanistic pathway, leading to the dissociation of two 1:1 complexes. In the sequential mechanism, the binding of the first metalloprotease molecule leads to destabilization of the DM43 homodimer, generating a 1:1 complex and a free DM43 monomer. The latter may either recombine with a second

DM43 monomer to form a new homodimer or, alternatively, complex with a second metalloproteinase molecule. In both cases, it seems reasonable to assume that the final complex has its dimerization surface at least either sterically hidden as a consequence of a conformational change or partially blocked by the enzyme molecule because no oligomeric intermediate with two inhibitor monomers and one enzyme molecule was detected. Although these are highly speculative proposals, the mechanisms presented here should, at the very least, provide a structural framework for the design of future experiments aimed at probing the mechanism of DM43 action in more detail. It is important to note that the model agrees with the inhibitor homodimeric structure through a dimerization surface on the D2 domain and accepts a 1:1 stoichiometry with the metalloproteinase.

A tempting proposition is to consider that these metalloproteinase inhibitors are part of the immune system, specifically the innate immune system, as are other soluble proteins like those of the complement cascade. Several experimental data point in this direction. 1) At the sequence level, there is a consistent homology between the amino acid sequences of DM43 and other molecules that belong to the natural immunity system, the KIRs. Additionally, Ig-like signatures are also found in DM43: disulfide bridges that link β-strands B and F and the aromatic residues originating in β-strand C. 2) At the conformational level, there is an Ig-like fold in DM43. 3) Functionally, the protection afforded by DM43 against foreign toxins indicates that these serum metalloproteinase inhibitors exert functions of the immune system.

In summary, DM43 is a dimeric glycoprotein that inhibits SVMPs by binding to their metalloproteinase domains at a 1:1 stoichiometry. It has three Ig-like domains that could be modeled after the KIRs. Data indicate that the binding of DM43 to SVMP could follow a concerted or sequential mechanism. It is proposed that this inhibitor class belongs to the innate immune system.

Acknowledgments—We thank Drs. José O. Previato and Lúcia Mendonça-Previato for performing the carbohydrate analysis. We are also grateful to Surza L. G. Rocha and Richard H. Valente for technical assistance.

REFERENCES

1. Domont, G. B., Perales, J., and Moussatché, H. (1991) *Toxicon* **29,** 1183–1194
2. Thwin, M. M., and Gopalakrishnakone, P. (1998) *Toxicon* **36,** 1471–1482
3. Dunn, R. D., and Broady, K. W. (2001) *Biochim. Biophys. Acta* **1533,** 29–37
4. Perales, J., and Domont, G. B. (2001) in *Perspectives on Toxinology* (Ménez, A., ed) John Wiley & Sons Ltd., London, in press
5. Mebs, D. (1998) in *Enzymes from Snake Venom* (Bailey, G. S., ed) pp. 1–10, Alaken, Inc., Fort Collins, CO
6. Rawlings, N. D., and Barrett, A. J. (1995) *Methods Enzymol.* **248,** 183–228
7. Primakoff, P., and Myles, D. G. (2000) *Trends Genet.* **16,** 83–87
8. Fox, J. W., and Long, C. (1998) in *Enzymes from Snake Venom* (Bailey, G. S., ed) pp. 151–178, Alaken, Inc., Fort Collins, CO
9. Stöcker, W., Grams, F., Baumann, U., Reinemer, P., Gomis-Ruth, F. X., McKay, D. B., and Bode, W. (1995) *Protein Sci.* **4,** 823–840
10. Kamiguti, A. S., Hay, C. R., Theakston, R. D., and Zuzel, M. (1996) *Toxicon* **34,** 627–642
11. Markland, F. S. (1998) *Toxicon* **36,** 1749–1800
12. Matsui, T., Fujimura, Y., and Titani, K. (2000) *Biochim. Biophys. Acta* **1477,** 146–156
13. Gomis-Ruth, F. X., Kress, L. F., and Bode, W. (1993) *EMBO J.* **12,** 4151–4157
14. Zhang, D., Botos, I., Gomis-Ruth, F. X., Doll, R., Blood, C., Njoroge, F. G., Fox, J. W., Bode, W., and Meyer, E. F. (1994) *Proc. Natl. Acad. Sci. U. S. A.* **91,** 8447–8451
15. Kumasaka, T., Yamamoto, M., Moriyama, H., Tanaka, N., Sato, M., Katsube, Y., Yamakawa, Y., Omori-Satoh, T., Iwanaga, S., and Ueki, T. (1996) *J. Biochem.* (*Tokyo*) **119,** 49–57
16. Gong, W., Zhu, X., Liu, S., Teng, M., and Niu, L. (1998) *J. Mol. Biol.* **283,** 657–668
17. Zhu, X., Teng, M., and Niu, L. (1999) *Acta Crystallogr. Sect. D Biol. Crystallogr.* **55,** 1834–1841
18. Hite, L. A., Jia, L. G., Bjarnason, J. B., and Fox, J. W. (1994) *Arch. Biochem. Biophys.* **308,** 182–191
19. Bjarnason, J. B., and Fox, J. W. (1995) *Methods Enzymol.* **248,** 345–368
20. Fox, J. W., and Bjarnason, J. (1998) in *Enzymes from Snake Venom* (Bailèy, G. S., ed) pp. 599–632, Alaken, Inc., Fort Collins, CO
21. Pérez, J. C., and Sánchez, E. E. (1999) *Toxicon* **37,** 703–728
22. Yamakawa, Y., and Omori-Satoh, T. (1992) *J. Biochem.* (*Tokyo*) **112,** 583–589
23. Valente, R. H., Dragulev, B., Perales, J., Fox, J. W., and Domont, G. B. (2001) *Eur. J. Biochem.* **268,** 3042–3052
24. Catanese, J. J., and Kress, L. F. (1992) *Biochemistry* **31,** 410–418
25. Qi, Z. Q., Yonaha, K., Tomihara, Y., and Toyama, S. (1994) *Toxicon* **32,** 1459–1469
26. Qi, Z. Q., Yonaha, K., Tomihara, Y., and Toyama, S. (1995) *Toxicon* **33,** 241–245
27. Melo, P. A., and Suarez-Kurtz, G. (1988) *Toxicon* **26,** 87–95
28. Moussatché, H., and Perales, J. (1989) *Mem. Inst. Oswaldo Cruz Rio J.* **84,** 391–394
29. Perales, J., Amorim, C. Z., Rocha, S. L., Domont, G. B., and Moussatché, H. (1992) *Agents Actions* **37,** 250–259
30. Perales, J., Moussatché, H., Marangoni, S., Oliveira, B., and Domont, G. B. (1994) *Toxicon* **32,** 1237–1249
31. Neves-Ferreira, A. G. C., Perales, J., Ovadia, M., Moussatché, H., and Domont, G. B. (1997) *Toxicon* **35,** 849–863
32. Neves-Ferreira, A. G. C., Cardinale, N., Rocha, S. L. G., Perales, J., and Domont, G. B. (2000) *Biochim. Biophys. Acta* **1474,** 309–320
33. Paine, M. J., Desmond, H. P., Theakston, R. D., and Crampton, J. M. (1992) *J. Biol. Chem.* **267,** 22869–22876
34. Fox, J. W., and Bjarnason, J. B. (1995) *Methods Enzymol.* **248,** 368–387
35. Allen, G. (1989) in *Sequencing of Proteins and Peptide*, (Burdon, R. H., and van Knippenberg, P. H., eds) 2nd Ed., pp. 95–99, Elsevier Science Publishers B. V., Amsterdam
36. Schägger, H., and von Jagow, G. (1987) *Anal. Biochem.* **166,** 368–379
37. Krutzsch, H. C., and Inman, J. K. (1993) *Anal. Biochem.* **209,** 109–116
38. Shevchenko, A., Wilm, O., Vorm, O., and Mann, M. (1996) *Anal. Chem.* **68,** 850–858
39. Altschul, S. F., Madden, T. L., Schaffer, A. A., Zhang, J., Zhang, Z., Miller, W., and Lipman, D. J. (1997) *Nucleic Acids Res.* **25,** 3389–3402
40. Berman, H. M., Westbrook, J., Feng, Z., Gilliland, G., Bhat, T. N., Weissig, H., Shindyalov, I. N., and Bourne, P. E. (2000) *Nucleic Acids Res.* **28**, 235–242
41. Barton, G. J., and Sternberg, M. J. E. (1987) *J. Mol. Biol.* **198,** 327–337
42. Previato, J. O., Gorin, P. A. J., Mazurek, M., Xavier, M. T., Fournet, B., Wieruszesk, J. M., and Mendonça-Previato, L. (1990) *J. Biol. Chem.* **265,** 2518–2526
43. Usami, Y., Fujimura, Y., Miura, S., Shima, H., Yoshida, E., Yoshioka, A., Hirano, K., Suzuki, M., and Titani, K. (1994) *Biochem. Biophys. Res. Commun.* **201,** 331–339
44. Pace, C. N., Vajdos, F., Fee, L., Grimsley, G., and Gray, T. (1995) *Protein Sci.* **4**, 2411–2423
45. Fan, Q. R., Mosyak, L., Winter, C. C., Wagtmann, N., Long, E. O., and Wiley, D. C. (1997) *Nature* **389,** 96–100
46. Sali, A., and Blundell, T. L. (1993) *J. Mol. Biol.* **234,** 779–815
47. Brooks, B. R., Bruccoleri, R. E., Olafson, B. D., States, D. J., Swaminathan, S., and Karplus, M. (1983) *J. Comp. Chem.* **4**, 187–217
48. Laskowski, R. A., MacArthur, M. W., Moss, D. S., and Thornton, J. M. (1993) *J. Appl. Crystallogr.* **26,** 283–291
49. Luthy, R., Bowie, J. U., and Eisenberg, D. (1992) *Nature* **356,** 83–85
50. Vriend, G., and Sander, C. (1993) *J. Appl. Crystallogr.* **6,** 47–60
51. Vriend, G. (1990) *J. Mol. Graphics* **8**, 52–56
52. Jones, S., and Thornton, J. M. (1997) *J. Mol. Biol.* **272,** 133–143
53. Ishioka, N., Takahashi, N., and Putnam, F. W. (1986) *Proc. Natl. Acad. Sci. U. S. A.* **83,** 2363–2367
54. Valiante, N. M., Lienert, K., Shilling, H. G., Smits, B. J., and Parham, P. (1997) *Immunol. Rev.* **155,** 155–164
55. Morris, A. L., MacArthur, M. W., Hutchinson, E. G., and Thornton, J. M. (1992) *Proteins Struct. Funct. Genet.* **12,** 345–364
56. Harpaz, Y., and Chothia, C. (1994) *J. Mol. Biol.* **238,** 528–539
57. Bazan, J. F. (1990) *Proc. Natl. Acad. Sci. U. S. A.* **87,** 6934–6938
58. de Vos, A. M., Ultsch, M., and Kossiakoff, A. A. (1992) *Science* **255,** 306–312
59. Somers, W., Ultsch, M., de Vos, A. M., and Kossiakoff, A. A. (1994) *Nature* **372,** 478–481
60. Bjarnason, J. B., and Fox, J. W. (1994) *Pharmacol. Ther.* **62,** 325–372
61. Black, R. A., and White, J. M. (1998) *Curr. Opin. Cell Biol.* **10,** 654–659
62. Amour, A., Slocombe, P. M., Webster, A., Butler, M., Knight, C. G., Smith, B. J., Stephens, P. E., Shelley, C., Hutton, M., Knäuper, V., Docherty, A. J., and Murphy, G. (1998) *FEBS Lett.* **435,** 39–44
63. Amour, A., Knight, C. G., Webster, A., Slocombe, P. M., Stephens, P. E., Knauper, V., Docherty, A. J., and Murphy, G. (2000) *FEBS Lett.* **473**, 275–279
64. Loechel, F., Fox, J. W., Murphy, G., Albrechtsen, R., and Wewer, U. M. (2000) *Biochem. Biophys. Res. Commun.* **278,** 511–515
65. Kashiwagi, M., Tortorella, M., Nagase, H., and Brew, K. (2001) *J. Biol. Chem.* **276,** 12501–12504
66. Maenaka, K., Juji, T., Stuart, D. I., and Jones, E. Y. (1999) *Structure* **7**, 391–398
67. Snyder, G. A., Brooks, A. G., and Sun, P. D. (1999) *Proc. Natl. Acad. Sci. U. S. A.* **A 96,** 3864–3869
68. Hood, L., Kronenberg, M., and Hunkapiller, T. (1985) *Cell* **40,** 225–229
69. Takeya, H., and Iwanaga, S. (1998) in *Enzymes from Snake Venom* (Bailey, G. S., ed) pp. 11–38, Alaken, Inc., Fort Collins, CO
70. Hutchinson, E. G., and Thornton, J. M. (1996) *Protein Sci.* **5**, 212–220

Structural and Functional Analyses of DM43, a Snake Venom Metalloproteinase Inhibitor from *Didelphis marsupialis* Serum

Ana G. C. Neves-Ferreira, Jonas Perales, Jay W. Fox, John D. Shannon, Débora L. Makino, Richard C. Garratt and Gilberto B. Domont

J. Biol. Chem. 2002, 277:13129-13137.
doi: 10.1074/jbc.M200589200 originally published online January 28, 2002
